FACTA UNIVERSITATIS
Series: **Mechanics, Automatic Control and Robotics** Vol.3, Nº 13, 2003, pp. 745 - 754

EVALUATION OF EDDY CURRENT SENSITIVITY FOR THE INSPECTION OF CRACK PROPAGATION UNDER A COMPOSITE PATCH

UDC 537.856 539.421

Zaira P. Marioli-Riga[1], George J. Tsamasphyros[2], George N. Kanderakis[2]

[1] Hellenic Aerospace Industry Ltd., R&D Department, Shimatari, Greece, 32009
E-mail: zmarioli@haicorp.com
[2] National Technical Univ. of Athens, Dept. of Eng. Science, Section of Mech. Athens, Greece, 15773

Abstract. *The increasing demand for life extension of both military and civilian aircrafts leaded to significant advances in repair technology of cracked metallic structures. Thus, composite patch repair of metallic structures became a rapidly grown technology in the field of aerospace. The eddy current method is used to trace crack propagation under a composite patch repair of a cracked metallic structure, after mechanical testing in fatigue. The capability and the reliability of the eddy-current method to detect cracks under a composite obstacle of significant thickness are checked for several patch thicknesses. Notched specimens 6mm thick were fabricated using 2024-T3 Aluminum. Boron Epoxy patches bonded with film adhesive were applied to the one side of the metallic specimens. Initial notches were 10mm long, while the thickness of the reinforcement was varying from 2 layers (0.25mm) to 7 layers (0.875mm) in order to represent actual structural composite patch repairs. Crack propagation from the tip of the notches was achieved by fatigue loads. The estimation of required loads to cause fatigue crack propagation was done by means of three-dimensional finite elements analysis. The eddy current method was then applied to trace the crack tip under the patch after their mechanical testing. Accuracy of the eddy-current method was verified by measuring the crack lengths on both sides of the specimen and comparing the results. The eddy-current method was found to be fully capable of tracing the crack propagation under the composite patch, requiring only proper calibration for the generator. Small differences in the crack lengths between the patched and the unpatched side of the specimen were explained by their non-symmetric configuration, which induced different stress intensity factors at the patched and the unpatched sides, as finite elements analysis has clearly shown.*

Key words: *Composite Patch Repair, Eddy-Current, Fatigue, Non Destructive Inspection, Composite Materials.*

Received October 20, 2002

1. INTRODUCTION

Present-day economic world conditions are forcing to the operation of both military and civilian aircraft well beyond their original design life, resulting in innovative repair techniques. As a result, one of them, the adhesively bonded composite patch repair of metallic aircraft components, is becoming a well-established technology. Adhesively bonded composite reinforcements offer remarkable advantages such as mechanical efficiency, repair time and cost reduction, high structural integrity, anticorrosion properties and inspectable damage tolerant repair. However, the thickness and the nature of the materials that form the patch may influence the quality and the accuracy of the non-destructive evaluation performed under it, especially in the case of a cracked substrate. Bonded repairs are mechanically efficient, cost effective and can be applied rapidly to produce an inspectable damage tolerant repair. Compared to metals advanced fiber composites have the advantages of formability, tailorability of stiffness, high specific strength and immunity to corrosion and fatigue. Composite patches can be precured and secondarily bonded on cracked structures or cocured in situ [1].

The greatest concerns with mechanical repairs are the danger of crack initiation from one of the new fastener holes as well as the difficulty in detecting this crack by standard Non Destructive Inspection (NDI) procedures, until the crack emerges from under the repair. The crack may initiate because of high stress concentrations (usually at the first row of fasteners) or because of poor quality hole drilling. The danger of crack initiation from hidden corrosion, which can develop under a poor mechanical repair also exists. On the other hand, the bonded patch, if correctly designed, has a relatively small influence on the stress field, so no crack initiation occurs in adjacent regions. Another significant advantage of composite patch repairs is the ability to tailor the geometry and the material properties of the patch to specific strength and stiffness requirements in order to achieve the desired reduction of stress intensity factors [2,3]. More data on design and application of composite patch repairs can be found in the corresponding references [4-8].

2. SPECIMEN CONFIGURATION – MATERIALS

The selection of the specimen configuration as well as the choice of the materials from which the specimens would be fabricated for this paper were driven by the cases of repairs usually met in the field of aeronautics technology, where composite patch repairs are usually applied. As a result, relatively thin (only 6mm thick) specimens made of Aluminum 2024-T3 were fabricated, representing an external aircraft's skin. The dimensions of the specimens were 360x65 mm, while 10mm notches were induced to them in order to enable crack initiation after fatigue loading. The Boron Epoxy patches were pre-fabricated in an autoclave using 5521 Textron prepreg. All the composite patches were unidirectional, which is the case met in most actual repairs, in order to coincide with primary loading direction. Their dimensions were 160x65 mm in order to cover the full notch length and to enable further propagation of the crack under them, while their thickness was from 2 layers (0.25mm) to 7 layers (0.875mm) to represent actual structural composite patch repairs. Composite patches were bonded over the cracked metallic specimens using FM73 high performance advanced film adhesive. The metallic specimens were initially surface treated using grit blasting and silane in order to ensure a reliable bonding of the patch over the specimen. The adhesive was cured at 120^{o} C for 1 hour to achieve the specified strength of the bonding.

It should be emphasized once more that all the materials and the procedures used for the fabrication of the specimens were similar to those applied for the composite patch repair of actual structures, in order to enable direct application of the results of this paper to real life repair requests. The basic characteristics of the materials used are presented in Table 1, while the dimensions and the initial notch lengths of the specimens are presented in Table2.

Table 1. Thickness and basic mechanical properties of the materials used

Material	Thickness (mm)	Tensile Modulus E_1 (MPa)	Tensile Modulus E_2 (MPa)	Shear Modulus (MPa)	Poisson Ration ν_{12}
Aluminum 2024-T3	6	72000	72000	26900	0.3
Textron 5521 Prepreg	0.125 per ply	207000	19000	4800	0.21
FM73 Film Adhesive	0.2	–	–	750	–

Table 2. Dimensions and initial crack lengths of the specimens

Specimen Number	Specimen Dimensions (mm)	Notch Length (mm)	Notch Width/ Specimen Length	Patch Dimensions (mm)	Number of Layers	Patch Thickness (mm)
1	360x65	10	0.15	160x65	2	0.25
2	360x65	10	0.15	160x65	2	0.25
3	360x65	10	0.15	160x65	4	0.5
4	360x65	10	0.15	160x65	4	0.5
5	360x65	10	0.15	160x65	7	0.875

3. ESTIMATION OF CRACK PROPAGATION

The required fatigue load was calculated numerically by using three-dimensional finite elements analysis. The finite element method is frequently used for the calculation and the design of a composite patch repair, as the most efficient, accurate and easy to apply numerical method. Two-dimensional and three-dimensional elements can be built for the calculation of stresses, strains, deflections and stress intensity factors before and after the application of the repair, in order to estimate the structural efficiency of the patch and calculate the remaining life of the component. Two-dimensional models are generally easier to build, but in most cases they cannot calculate the required results with high accuracy, especially in complicated cases (complex geometry, big thickness variations etc.). On the other hand, three-dimensional models can cope for all these peculiarities providing relatively accurate results, but demand higher modeling effort and computational resources. In this paper, three-dimensional finite elements models were created using the ANSYS standard finite elements code, in order to achieve more accurate results for better comparison with the experimental results. One layer of three-dimensional SOLID 95 structural solid elements (common 20-node three-dimensional elements having three degrees of freedom at each node in translations in the nodal x, y and z directions [9]) were used to model each different material (metallic plate, adhesive layer and composite patch). The elements can, among other, support orthotropic materials, as in the case of the composite patch, as well as temperature loads. Connectivity of the elements was established by using common nodes at the interface of the elements (the upper nodes of the metallic plate were common with the lower nodes of the adhesive, whereas the upper nodes of the adhesive were identical with the lower nodes of the composite patch). The thickness and the material properties introduced for each layer corresponded to the thickness and the properties of the actual materials used as well as to the specimen configuration. Only 1/2 of the actual repair was modeled because of symmetry and the required symmetry boundary conditions were applied at the edges of the model in all cases. Different models were built according to the variations in patch thicknesses. The three-dimensional model for the 2-layers configuration are shown generally and in detail in Figures 1 and 3. The crack was modeled by leaving the related edge nodes of the metallic substrate unconstrained, while the nodes of the composite patch were properly connected to the rest of the material. The force was applied as pressure far away from the repair to ensure that the area of interest is beyond any transition effects. Very fine singular elements were used in the first row of elements next to the crack tip in order to calculate the stress intensity factor. Normal 20-node elements were transformed to singular elements by moving the midside node to the 1/4 of the element side towards the crack tip. The stress intensity factor at the crack tip was computed using the displacement method by means of the formula [9]:

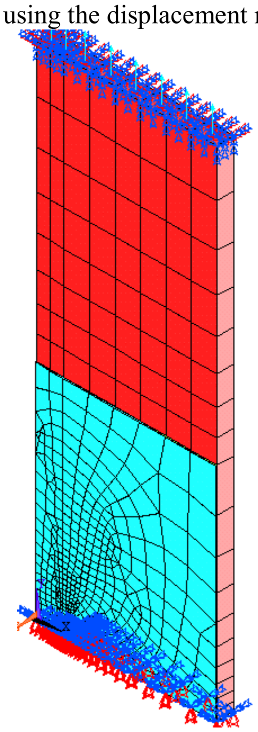

Fig. 1. Overview of the three–dimensional model

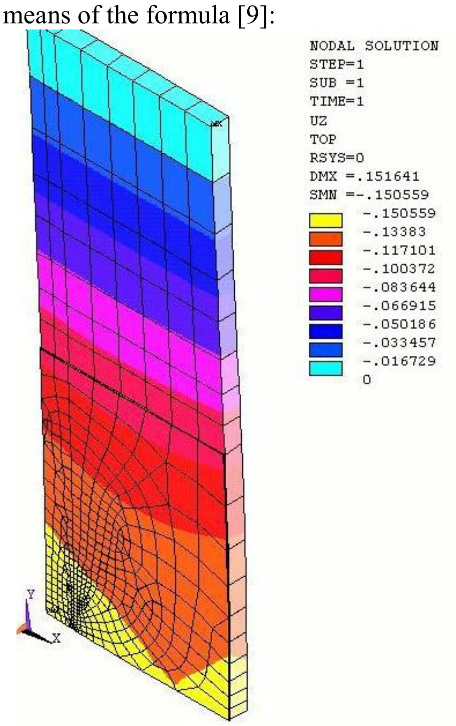

Fig. 2. Out-of-plane displacement

$$K_I = \sqrt{2\pi}\,\frac{2G}{1+\kappa}\,\frac{|v|}{\sqrt{r}} \qquad (1)$$

where: $|v|$, is the displacement in the local Cartesian system.
r, denotes the coordinates in the local cylindrical system.
G, is the shear modulus of the cracked material.
$\kappa = (3 - n) / (1 + n)$ for plane stress.
and n, stands for the Poisson ratio.

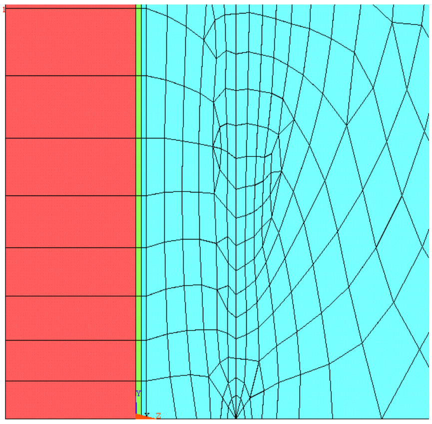

Fig. 3. Detail of the different layers and the crack modeling.

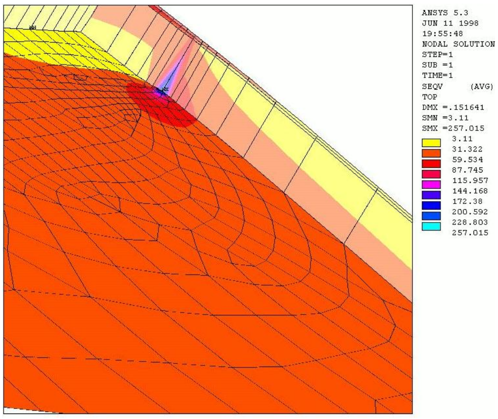

Fig. 4. Through-the-thickness Von Mises stresses developed in the area of the crack

Having had calculated the stress intensity factor at the crack tip under the composite patch, the remaining life of the specimen and the crack propagation rate were calculated using the Paris law [10]:

$$da / dN = C(\Delta K)^m \qquad (2)$$

In order to calculate the increase of the remaining life of the structure, the stress intensity factor of the unpatched specimen was as well calculated and was compared with the corresponding values of the patched specimens. Assuming that the exponential coefficient of (2) for Aluminum is m = 3, composite patching of the specimens was found to result in an increase of the remaining life by a factor of 6 to 10, according to the number of boron layers used for the patch. Based on the computed results it was estimated that a remote load of 60000N would be capable to cause crack propagation of around 10mm in about 10000cycles, which was a reasonable crack length for the examination of the reliability of the eddy-current method, under different composite obstacles. Nevertheless, it should be stressed that two side effects were revealed by finite elements analysis, because of the non-symmetric configuration of the specimens. The first, was the out-of-plane displacement of the specimens in uniaxial loading, because of the single side reinforcement applied, as shown in Figure 2. The second, were the big differences in the calculated stress intensity factors between the unpatched and the patched side of the specimen, as it can be qualitatively shown by the difference in the corresponding developed stresses at the crack tip at Figure 4. All the calculated results from the finite elements analysis (out-of-plane displacements and stress intensity factors) are presented ion Table 3.

4. EXPERIMENTAL PROCEDURE

The specimens were loaded by means of an INSTRON 8501 fatigue loading machine. Tension – tension loads between 2000N and 60000N (corresponding to 154MPa maximum remote stress) was applied to all specimens with 1Hz frequency. Minimum load was chosen to be slightly higher than zero in order to avoid possible compression loading because of late response of the machine control unit or from inertia effects. The crack propagation as well as the out-of-plane displacement were measured every 1000 cycles. Crack measurements were taken while the specimen was fully loaded, when the whole length of the crack was revealed. On the contrary, the reference point (zero point) for the out-of-plane displacement measurement was taken every time with the specimen unloaded, and the displacement was then measured by loading the specimen to 60000N. The final results of all the measurements are shown in Table 3.

After the fatigue loading process NDI was performed by means of an NORTEC NDT-25L eddy current generator, using a 100Hz probe. Crack lengths were calculated by measuring the distance between the point which the eddy-current method indicated as crack tip and the edge of the specimen. Initially the instrument was calibrated for the NDI of the unpatched sides, using an angle of 283^{o}, Gain = 48 (24dB), Filter = 0, $V_{sensitivity} = 0.2$ and $H_{sensitivity} = 1$. The waveform produced because of the cracks is shown in Figure 5, while the measured crack lengths are presented in Table 3.

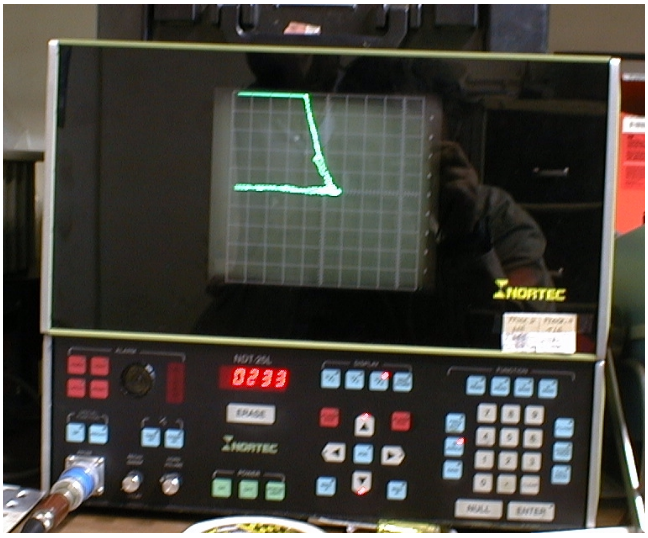

Fig. 5. Waveform produced by the crack measured at the unpatched side of the specimen

The calibration of the instrument for the NDI above the boron patch was achieved by using a patched aluminum plate with cracks of known length under the boron patch. The produced waveform for the different crack lengths (0.5mm, 1mm and 2mm) is shown in Figure 6. The angle varied according to the number of layers of the patch (226^{o} for 2 layers, 223^{o} for 4 layers and 219^{o} for 7 layers) while the rest of the parameters were kept to their original values. . The waveform produced at the crack tips under the boron patch is shown in Figure 7 while the measured crack lengths are presented in Table 3.

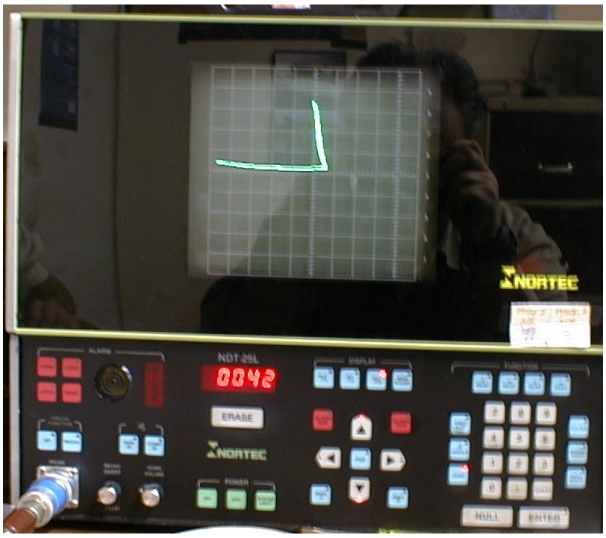

Fig. 6. Waveform produced by the crack measured at the patched side of the specimen (measured under the boron patch).

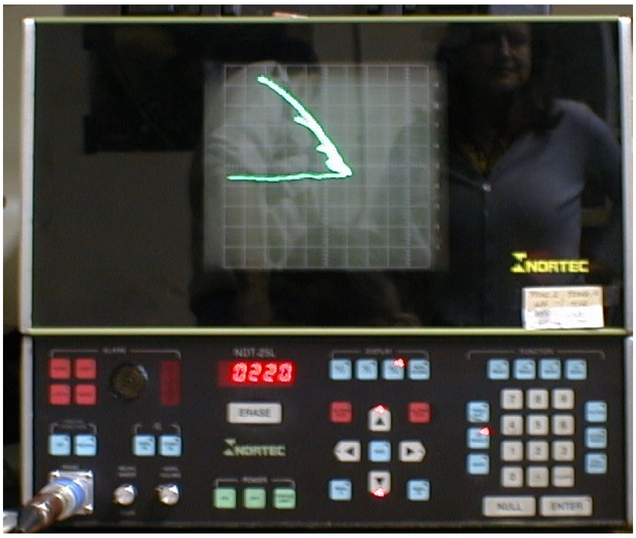

Fig. 7. Waveform produced by the three different cracks (0.5mm, 1mm and 2mm) above the boron patch of the calibration specimen

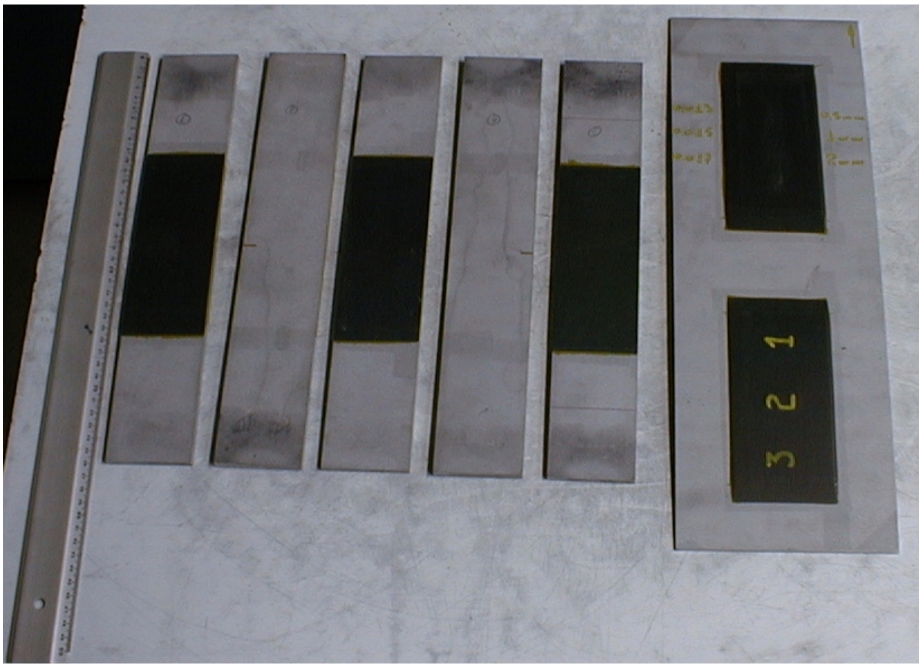

Fig. 8. Specimens manufactured (on the left) and calibration specimen (on the right)

Table 3. Experimental and numerical results

Specimen Number	Patch Thickness (mm)	Out-of-plane Displacement FEA (mm)	Out-of-plane Displacement Experimental (mm)	Stress Intensity Factor Patched Side	Stress Intensity Factor Unpatched Side	Crack length Patched Side (mm)	Crack length Unpatched Side (mm)	Number of Cycles
1	0.25	0.64	0.56	684.2	1309.4	20	22	11000
2	0.25	0.64	0.56	684.2	1309.4	20	22	7500
3	0.50	0.92	1.01	626.8	1315.1	22	27	11000
4	0.50	0.92	1.075	626.8	1315.1	22	27	8000
5	0.875	1.18	1.26	589.9	1318.3	22	24	10500

The crack lengths measured above the patch were compared with the corresponding crack lengths measured from the non-patched side of the specimen. As obviously shown in Table 3 the crack lengths at the unpatched side were slightly higher than the ones measured at the patched side. Again, this was predicted from the finite elements analysis, by the different values of the stress intensity factor at the two sides of the specimen, which resulted in different crack propagation rates.

5. Conclusions - Summary

A major project is running in order to check the capability, the sensitivity and the reliability of the eddy-current method to detect cracks under a composite obstacle of significant thickness. The results of this project will be used for the calculation of the remaining life of composite patch repaired structures and the definition of inspection intervals using the eddy-current method, according to the damage tolerance analysis. For this purpose notched specimens were fabricated using Aluminum 2024-T3, and Boron Epoxy patches were bonded to the one side of the metallic specimens using film adhesive. The specimens were then submitted to cyclic loading. According to the experimental results, the eddy-current method has been proved to be capable of detecting cracks under boron-epoxy composite patches fabricated from up to 7 layers (0.875mm thick). The differences of the measurements between the patched and the unpatched side are not due to lack of sensitivity of the eddy-current method but are explained by the non-symmetric way of crack propagation due to the non-symmetric configuration of the specimens. This was proven both analytically using the finite elements method, experimentally by the out-of-plane displacement measured and by X-rays of the cracked area after the eddy-current inspection. It should be noted that the difference of the stress intensity factor at the two sides of the patch computed by finite elements analysis, should theoretically result in higher differences of crack lengths. However, the numerical results correspond to the initial stage of crack growing, when the crack is vertical to the patch, while a different angle is expected after some loading because of the differences in the crack propagation rates. Nevertheless, it should be noted that appropriate calibration of the eddy-current generator is required before each different thickness is measured. Further work will be performed in order to investigate accuracy of the method for thicker patches, to verify the minimum detectable crack length for every patch thickness and to decide on the ability of the method to detect plasticity or other cases of damage under a boron-epoxy composite patch, before a crack has initiated.

References

1. Baker A.A., Bonded Composite Repair of Metallic Aircraft Components – Overview of Australian Activities, AGARD, CP-550.
2. Z.P. Marioli-Riga, G.J. Tsamasphyros, G.N. Kanderakis, Development of a Method for A/C Emergency Repairs by Composite Patches, S.A. Paipetis, E.E. Gdoutos, (Xanthi1997), Vol II 143-156
3. Duong C.N., Yu J., The Stress Intensity Factor for a Cracked Stiffened Sheet Repaired with an Adhesively Bonded Composite Patch, International Journal of Fracture 84(1997), p. 37-60
4. Baker A.A., Jones R., Bonded Repair of Aircraft Structures, Martinus Nijhoff Publishers, Dordrecht, (1988).
5. Composite Repairs of Cracked Metallic Airframe Structures, U.S. Department of Transportation, Federal Aviation Administration, CT-92/32 (May 1993).
6. G.J. Tsamasphyros, G.N. Kanderakis, Z.P. Marioli-Riga, Three-dimensional Finite Elements Analysis of Debonding and Thermal Effects Near the Crack-Tip of a Metal Structure Repaired by a Composite Patch, 5th National Congress on Mechanics, University of Thessaly, Greece, June 1999.
7. Fredell R., Mazza J., Fatigue in New and Ageing Aircraft – The Development of an Integrated Bonded Repair System, 19 International Committee on Aeronautical Fatigue Symposium, Edinburgh, Scotland, (June 1997).
8. Applications of Fracture Mechanics to the Durability of Bonded Composite Joints, DOT/FAA/AR-97/56 (May 1998).
9. ANSYS Finite Elements Analysis Programme, Theory Manual
10. Parker A.P., The Mechanics of Fracture and Fatigue, E&F.N. Spon Ltd, 1981, London & NY.

OCENA OSETLJIVOSTI NA VRTLOŽNU STRUJU KOD NADGLEDANJA PROSTIRANJA PRSLINE POD MEŠOVITOM ZAKRPOM

Zaira P. Marioli-Riga, George J. Tsamasphyros, George N. Kanderakis

Rastuća potreba za produženjem trajanja kako vojnih, tako i civilnih vazduhoplova dovela je do značajnih pomaka u tehnologiji popravke naprslih metalnih struktura. Time je popravka metalnih struktura mešovitim krpljenjem postala tehnologija koja se naglo razvija u oblasti avioprostora. Metoda vrtložne struje koristi se za praćenje prostiranja prsline kod opravke mešovitim krpljenjem naprsle metalne strukture, nakon mehaničkog testiranja na zamor. Sposobnost i pouzdanost metode vrtložne struje u otkrivanju prsline pri mešovitoj smetnji značajne debljine provereni su za nekoliko različitih debljina zakrpe. Zarezani uzorci debljine 6mm proizvedeni su korišćenjem 2024-T3 aluminijuma. Borne Epoksi zakrpe spojene slojnim vezivnim sredstvom primenjene su na jednu stranu metalnih uzoraka. Početni zarezi bili su dugi 10mm, dok je debljina ojačanja varirala od 2 sloja (0,25mm) do 7 slojeva (0,875mm) da bi se prikazale stvarne popravke modela mešovitim krpljenjem. Prostiranje prsline od vrha zareza ostvareno je opterećenjima do zamora. Procena opterećenja potrebnih da se izazove prostiranje prsline usled zamora uradjena je putem trodimenzionalne analize konačnih elemenata. Potom je metoda vrtložne struje primenjena da se prati vrh prsline ispod zakrpe nakon njihovog mehaničkog testiranja. Preciznost metode vrtložne struje potvrdjena je merenjem dužine prslina na obe strane uzorka i poredjenjem rezultata. Nadjeno je da je metoda vrtložne struje u potpunosti u stanju da prati prostiranje prsline pod mešovitom zakrpom, pri čemu je samo neophodno odgovarajuće kalibrovanje generatora. Manje razlike u dužini prslina izmedju krpljene i nekrpljene strane uzorka objašnjene su njihovom nesimetričnom konfiguracijom, koja je izazvala različite faktore intenziteta napona na krpljenoj i nekrpljenoj strani, kao što je to jasno pokazala analiza konačnih elemenata.